INTERNATIONAL ATOMIC ENERGY AGENCY
UNITED NATIONS EDUCATIONAL, SCIENTIFIC AND CULTURAL ORGANIZATION
INTERNATIONAL CENTRE FOR THEORETICAL PHYSICS
I.C.T.P., P.O. BOX 586, 34100 TRIESTE, ITALY, CABLE CENTRATOM TRIESTE

H4-SMR 393/68

SPRING COLLEGE ON PLASMA PHYSICS

15 May - 9 June 1989

ROTATING MAGNETIC FIELD CURRENT DRIVE AND ITS APPLICATION IN THE ROTAMAK: EXPERIMENTAL ASPECTS

I. R. Jones

School of Physical Sciences
The Flinders University of South Australia
Bedford Park
Australia

ROTATING MAGNETIC FIELD CURRENT DRIVE AND ITS APPLICATION IN THE ROTAMAK: EXPERIMENTAL ASPECTS

Ieuan R. Jones
School of Physical Sciences
The Flinders University of South Australia
Bedford Park, S.A. 5042
Australia

ABSTRACT

This paper presents general observations on the construction of rotamak devices, a description of the diagnostics which are employed (with particular emphasis on the use of Hall probes and the analysis of the data obtained with them) and discusses some experimental results of general validity. It finishes with an indication of future trends in rotamak research.

1. INTRODUCTION

This paper deals with the experimental aspects of applying the rotating magnetic field (RMF) current drive technique to the generation of a compact torus configuration.

The rotamak[1)] is a compact torus device in which a rotating magnetic field (rotating in planes normal to the z-axis; see Fig. 1) is used to generate and maintain the toroidal plasma current. Equilibrium requires an additional, externally generated, poloidal field (the so-called 'vertical field' of the tokamak) to counteract the natural tendency of the toroidal plasma ring to expand. The steady component of the resultant poloidal magnetic field consists of the combination of closed and open field lines shown in Fig. 1.

The paper presents general observations on the construction of rotamak devices, a description of the diagnostics which are employed (with particular emphasis on the use of Hall probes) and the analysis of the data obtained with them and discusses some experimental results of general validity. It finishes with an indication of future trends in rotamak research.

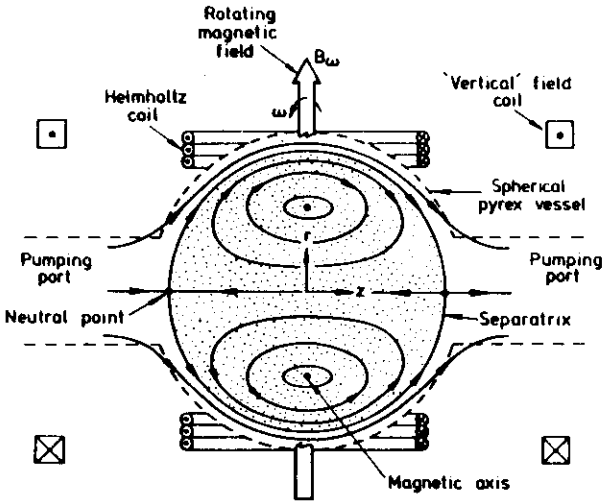

Fig. 1 The Rotamak compact torus configuration.

2. THE COMPONENTS OF A ROTAMAK DEVICE

The components of a typical rotamak device are show in Fig. 2. A discussion of the various parts follows.

2.1 Vacuum Vessels

Most rotamak experiments have been undertaken in glass (pyrex) vacuum vessels of spherical and cylindrical shapes. The first reported rotamak device[2)] used a spherical pyrex vessel of radius 6.4 cm while the latest version being constructed at Flinders University incorporates a pyrex cylinder (QVF-CORNING), 80 cm in length and 30 cm in radius. These vessels are furnished with pumping ports which connect them to conventional vacuum systems and with various entry ports which allow the introduction of electric and magnetic probes and the placement of Rogowski current belts.

It has already been recognized that in its eventual reactor

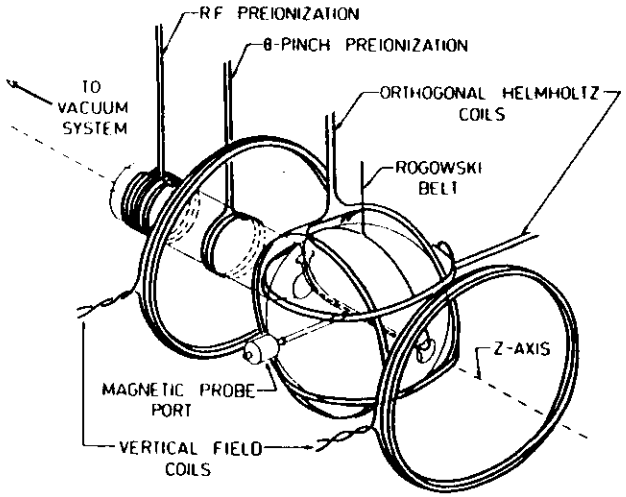

Fig. 2 Schematic diagram of a typical rotamak device.

embodiment, the rotamak discharge will most probably need to be generated within a metal vacuum chamber. Recently, the first experimental results obtained with such a vessel were reported[3].

2.2 Generation of the Rotating Magnetic Field

2.2.1 The RMF coil structure. In an ideal RMF current drive experiment, the steady electron current would be driven by means of an uniform rotating field. Such a field with the components:

$$B_r = B_\omega \cos(\omega t - \theta)$$
$$B_\theta = B_\omega \sin(\omega t - \theta)$$

can be generated in an interior region, $r \leq a$, by the continuous surface current distribution:

$$j_z(r,\theta,t) = - j_{zo}\, \delta(r - a) \sin(\omega t - \theta) .$$

Here, B_ω and ω are the amplitude and angular frequency of the RMF. The quantities j_{zo} and a are respectively the amplitude and radius of the current sheet.

In practice, a current sheet of the above form cannot be produced and, in long, cylindrical rotamak devices, it is approximated by a finite number of longitudinal dipole coils carrying polyphase currents. This results in an inhomogeneous magnetic field which deforms as it rotates. By a suitable choice of coil geometry and current phasing, this distortion can be kept to an acceptable value.

As an example of RMF coil design, we consider the coil structure used by Knight[4] in a cylindrical rotamak device. A diagram of the rotating field coils used in this experiment is shown in Fig. 3. For theoretical purposes, the coil structure is considered to be made up of a set of infinitely long dipoles carrying appropriately phased currents. The magnetic field produced by the *single* dipole shown in Fig. 4 can be written in the form,

$$\underline{B} = \nabla \times \underline{A} ,$$

where $\underline{A}$ is the magnetic vector potential. The vector potential at a point $P(r,\theta)$ for this (infinitely long) single dipole has only one component, A_z, which is given by

$$A_z(r,\theta) = \frac{\mu_o I}{4\pi} \ell n \left[\frac{1 + (r/R)^2 + 2(r/R) \cos(\theta - \phi)}{1 + (r/R)^2 - 2(r/R) \cos(\theta - \phi)} \right]$$

where I is the current in the dipole, R is its radius and ϕ is its angular position relative to a $\theta = 0$ datum.

The coil structure shown in Fig. 3 can be considered to be the superposition of eight dipoles located at the following values of ϕ and carrying the indicated currents:

$\phi_1 = -28°$	$I_1 = I_o \cos \omega t$
$\phi_2 = -17°$	$I_2 = I_o \cos \omega t$
$\phi_3 = 17°$	$I_3 = I_o \cos \omega t$
$\phi_4 = 28°$	$I_4 = I_o \cos \omega t$
$\phi_5 = 62°$	$I_5 = I_o \sin \omega t$
$\phi_6 = 73°$	$I_6 = I_o \sin \omega t$
$\phi_7 = 107°$	$I_7 = I_o \sin \omega t$
$\phi_8 = 118°$	$I_8 = I_o \sin \omega t$

The vector potential at P can be calculated by summing vector potentials

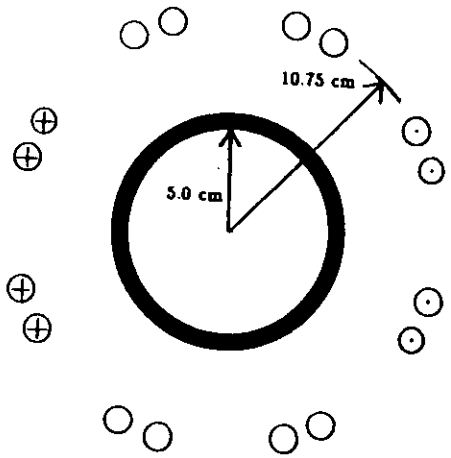

Fig. 3 Positions of the rotating field coils in KNIGHT[4] experiment.

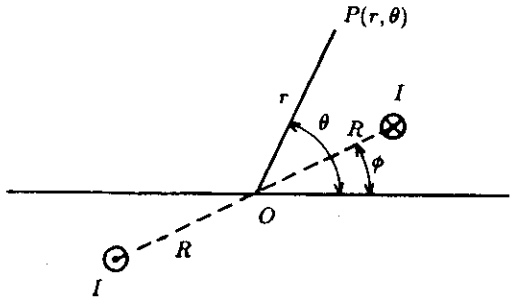

Fig. 4 A single dipole.

of the above form over these eight values of ϕ and I:

$$A_z(r,\theta,t) = \frac{\mu_o}{4\pi} \sum_{i=1}^{8} I_i \ell n \left[\frac{1 + (r/R)^2 + 2(r/R) \cos(\theta - \phi_i)}{1 + (r/R)^2 - 2(r/R) \cos(\theta - \phi_i)} \right]$$

In general, magnetic field lines can be calculated by finding a scalar function, f, such that

$$\underline{B} \cdot \nabla f = 0 .$$

Contours of equal values of f will then depict the field lines. For this case of an infinitely long coil structure, $f = A_z$. Fig. 5 shows

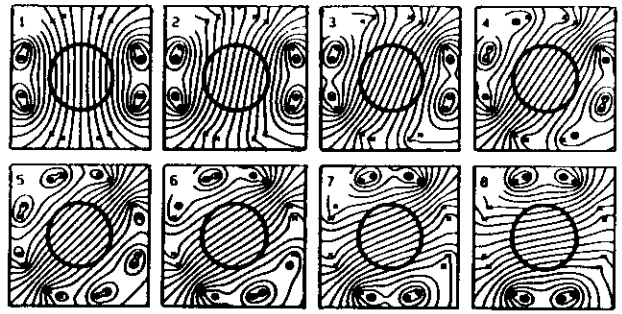

Fig. 5 Rotating field lines for coil structure shown in Fig. 3.

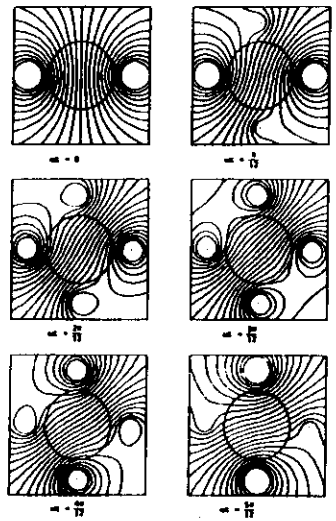

Fig. 6 Rotating field lines for a coil structure having one coil per phase.

the magnetic field lines (contours of A_z) for the coil structure under consideration. The lines are shown at a sequence of time steps during a quarter of a revolution. The steps are separated by 1/32nd of a period. Symmetry considerations provide the remaining time steps by simple rotations of those shown. The thick circle indicates the discharge vessel and it can be seen that the inhomogeneity of the rotating field over this region is quite small.

By way of contrast, Fig. 6 shows the field lines of the RMF when it is generated by the simplest coil structure consisting of a pair of orthogonal longitudinal dipole coils carrying RF currents which are dephased by 90°.[5] Considerable distortion of the field lines is observed.

Hugrass[6] has investigated the effect of spatial harmonics of the applied RMF on the overall efficiency of current drive. He concludes that the effect of spatial harmonics can be minimized by increasing the diameter of the coils with respect to the plasma diameter, carefully designing the coil structure to eliminate the fifth spatial harmonic and using a three-phase system to generate the RMF.

The reader should be aware that the above comments are applicable to long, cylindrical rotamak devices. No comparable study has been made of the optimum coil structure for spherical vessels. For the most part, two orthogonal Helmholtz coils have been used to produce the RMF in such rotamaks (see Fig. 2).

2.2.2 The RF power supplies. In order to generate the RMF, two RF current pulses of the same amplitude and frequency, but dephased by 90°, must be fed to the two orthogonally oriented coils which make up the coil structures described in the last section. The power supplies which furnish these current pulses are the most important, and usually the most expensive, component of a rotamak device. Since 1979, rotamak experiments have used the following types of RF generators

- RF line generators.[7] These provide high power (~ MW), short duration (~ μsecs) RF (~ 0.3 MHz) pulses and were used in the first series of rotamak experiments[2,8] (1979-1982).
- conventional vacuum tube RF generators. In a series of rotamak experiments undertaken at Flinders University and the Australian Nuclear Science and Technology Organization (ANSTO)[9,10] during the period 1982-1988, units of this type were used as a source of RF power. Typically, RF (1.0 MHz) pulses of 20-40 msec duration and at a power level of up to ~ 30 kW/channel were available.
- MOSFET (Metal oxide semiconductor field effect transistor) generators. This relatively new technology enables RF pulses of an appropriate frequency (0.1 - 1.0 MHz) and duration (~ 40 msec) to be generated at power levels of up to 10 kW/channel. They possess the great advantage of being relatively straightforward to construct and are reasonably priced.
- a combination of MOSFET and conventional vacuum tube RF generators. By combining a MOSFET generator as a driver stage and high power triodes (MACHLETT ML-8772) in a push-pull output stage, it has been possible to arrive at a high RF power level (400 kW/channel) in just two stages in the latest rotamak apparatus being constructed at Flinders University. The RF frequency is 0.5 MHz and the pulse duration is 40 msec. The power supply for the RF generator is a capacitor bank and, normally, the amplitude of the RF pulse would decrease during the period of the pulse. By programming the output of the MOSFET driver stage, however, it has been possible to compensate for the droop in the HT supply and flat-top RF pulses have been produced.

2.2.3 RF matching circuit. In order to transfer the maximum amount of power from the generators to the rotamak plasma, it is necessary to incorporate a matching circuit between each RF generator and the corresponding rotating field coil. The purpose of this circuit is to transform the highly inductive impedance of the RMF coil structure to one which is closer to the internal impedance of the generators. Fig. 7 shows the matching circuit which has been used with success at both Flinders University and ANSTO over the past 10 years. An investigation of alternative matching circuits has not been undertaken. The load consists of the rotating field coil inductance, L_c, the RF resistance of the coil, R_c, plus any extra loss in the circuit due to the presence

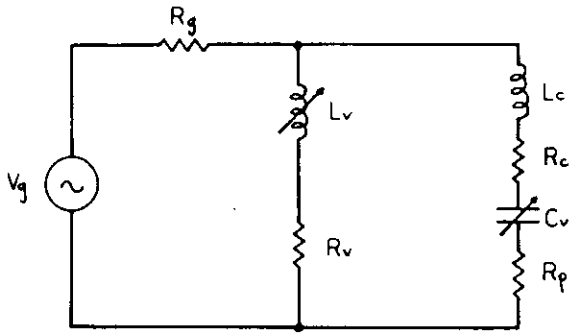

Fig. 7 The matching circuit.

of the plasma (the reflected resistance of the plasma), R_p. The matching circuit elements consist of a variable capacitor, C_v, connected in series with L_c and a variable inductor, L_v, of RF resistance, R_v, connected in parallel with the L_c and C_v. The principle of operation is that C_v is first tuned to make the plasma branch of the circuit slightly capacitative. Then the value of L_v is adjusted until it resonates with the plasma branch. In this way, high circulating currents are produced in the parallel tuned circuit.

In certain circumstances, the RF voltages across C_v and L_c are sufficient to cause breakdown between the turns of the rotating field coil and across the matching capacitor. This problem can be circumvented by distributing the matching capacitance along the plasma branch. This is achieved by using N matching capacitors, each of capacitance equal to NC_v, and placing them in between segments of the rotating field coil, each segment having an inductance of L_c/N. In this way, the maximum RF voltage appearing in the plasma branch is reduced to manageable proportions.

2.3 The Equilibrium (or 'Vertical') Magnetic Field.

The additional magnetic field which is required for plasma equilibrium is produced in spherical rotamak devices by a pair of coils (see Fig. 2) or, in the case of highly elongated rotamak discharges, by a solenoid surrounding a cylindrical vessel. The current pulses which feed these coils are derived from circuits which allow the rise-time, amplitude and duration of the pulses to be independently adjustable.

The shape of the separatrix of the rotamak discharge can be controlled by appropriately shaping the initially imposed equilibrium field. This is easily done by changing the positions of the equilibrium field coils.

2.4 Preionization

Preionization is usually achieved by passing a pulse of RF current (~ 20 MHz; ~ 1 sec pulse duration) through coils wound around the pumping ports of the discharge vessel. If the filling pressure is sufficiently high, or if the amplitude of the applied RMF is sufficiently large then it is often found that preionization is not required; the electric field associated with the RMF will bring about breakdown of its own accord.

3. DIAGNOSTICS

3.1 Total Driven Toroidal Plasma Current.

The most basic quantity that can be measured in a rotamak experiment is the total amount of toroidal plasma current which is driven by the applied RMF. This is measured by means of a Rogowski coil which is located as shown in Fig. 8 for a spherical rotamak device. It surrounds

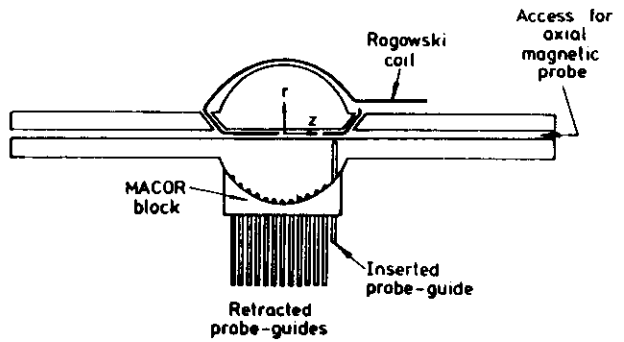

Fig. 8 Disposition of Rogowski coil and magnetic probe ports in a typical rotamak device.

a semi-circular cross section of the vessel and measures the total current threading it.

3.2 Magnetic Field Measurements

One of the principal diagnostics used in all rotamak experiments is magnetic probes. The density and temperature of rotamak discharges have (to date) allowed probes to be completely inserted into the plasma. Fig. 8 shows the disposition of the numerous magnetic probe guides which are incorporated into the design of a typical rotamak apparatus. The study of the internal magnetic fields can yield important information about several plasma parameters. In particular, it allows such quantities as the plasma current density and magnetic flux to be derived.

A distinguishing feature of the rotamak discharge is that a time-varying (rotating) magnetic field is used to produce a configuration which is quasi-static. One can therefore decompose the total magnetic field into a steady part and a part which oscillates in time. Two different types of magnetic probes are used to measure these components. A probe based on the Hall effect is used to measure the steady part of the field, while small inductive pick-up coils are used to measure the oscillating (RF) component.

We present here a detailed description of a Hall probe system since their use in plasma physics laboratories is not yet universal. On the other hand, the construction and use of miniature wire-wound magnetic probes is well-established.

3.2.1 Hall probes. The long time scale and comparatively small amplitude of the steady magnetic field component (40 msec and a few tens of gauss) of a rotamak discharge preclude the use of conventional miniature wire-wound coils. Instead, it is customary in the experiments at Flinders University and ANSTO to use a Hall element to obtain a signal proportional to the magnetic field. The element we have used is a SIEMENS SBV 566 Hall generator. The sensitive area is 0.9 mm x 0.9 mm square. The output of the element depends on the product of the control current and the magnetic flux through the probe. To obtain a signal proportional to the magnetic field, care is taken to ensure that the control current is held constant. The maximum control current specified for these elements is 50 mA. However, to enable reliable probe operation within the rather harsh plasma environment, a somewhat smaller control current of 15 mA is usually chosen. This current is obtained from the feedback controlled regulator circuit shown in Fig. 9(a). The circuit is powered by a pack of eight rechargeable Ni Cd batteries which can supply the Hall probe for a day's experimentation before requiring recharging. The supply circuitry is located in a grounded box which is connected to the Hall element via a 3 mm diameter stainless steel tube. The control current leads and the signal leads are twisted together and fed through this tube which both rigidly supports the element and acts as an electrostatic shield (see Fig. 9(b).

The output from a Hall probe is transmitted to a Faraday cage through 50Ω triaxial cable. The signal leads are connected to the centre and middle conductors of the cable and the outer shield is connected to the earthed Faraday cage. The raw probe output usually contains sufficient RF pick-up to necessitate the use of a low pass filter. It is then usually necessary to amplify the Hall probe signal by a factor of about fifty in order to improve the resolution when digitising. The complete Hall probe signal processing which is typically needed in rotamak experiments is illustrated in Fig. 9(c).

Hall probes are calibrated by inserting them into the centre of a Helmholtz coil of known geometry, carrying a known current. The linearity of these probes is excellent over the range of field strengths of interest (typically a few tens of gauss).

3.3 Other Diagnostics

A Hall probe system has been described in detail. The remaining diagnostic techniques used in rotamak experiments are straightforward and conventional

- a measurement of local plasma density and temperature by means of floating double Langmuir probes.[11] The density measurements are normalized by comparing them with a line-averaged density measurement obtained with an 8 mm microwave interferometer.

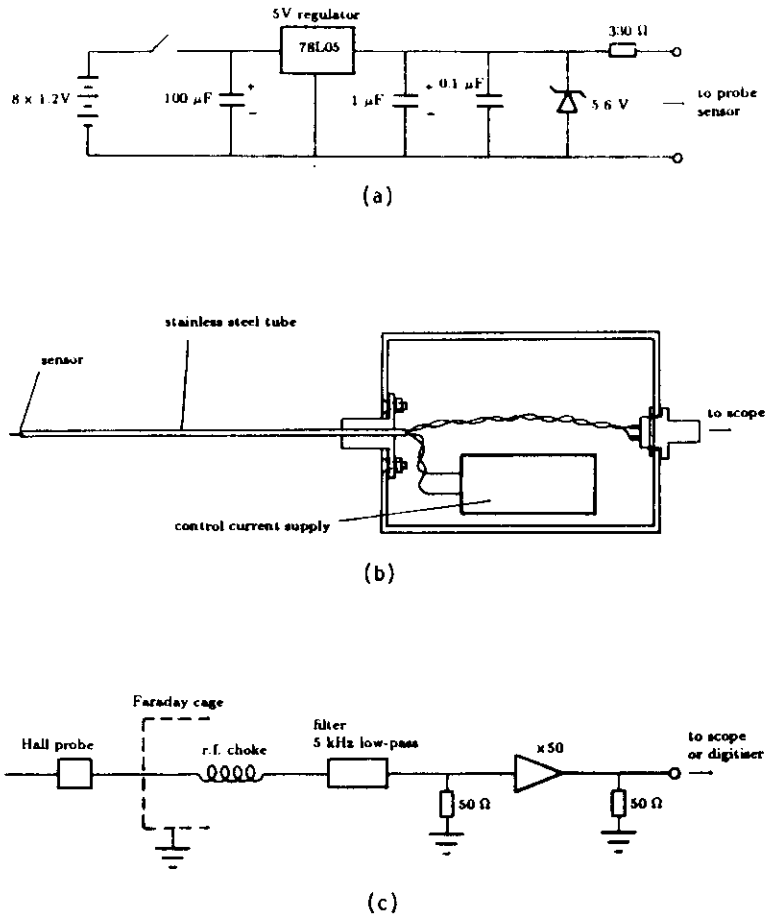

Fig. 9 The magnetic Hall probe system

(a) Control current supply

(b) Complete Hall probe

(c) Signal processing system.

- RF power measurements made by using voltage dividers and current transformers.
- a measurement of the total H_α emission which, when combined with the measurement of electron density, yields an estimate of the particle confinement time τ_p.

During many experimental runs the data from a plasma shot is stored on the screen of a digital storage oscilloscope and examined after the shot. Alternatively, the data is recorded permanently by taking a photograph of the screen on polaroid film. However, for major experimental runs involving many thousand successive discharges, the data is digitised and stored on computer disks for subsequent analysis.

4. EXPERIMENTAL RESULTS

In this section, experimental results of general validity will be presented. We stress that the results shown here do not come exclusively from one particular rotamak experiment; rather, they have been extracted from the sum total of results obtained in a variety of experiments involving rotamak discharges of different shapes and different RF input power.

4.1 The Generation of a Rotamak Discharge.

The generation of a typical rotamak discharge involves the following procedures

- the discharge vessel is evacuated to a base pressure of about 10^{-6} Torr,
- the filling gas (argon and hydrogen have been used in the Flinders University and ANSTO experiments) is allowed to flow continuously through the vessel, the flow rate being adjusted with a needle leak valve. The pressure of the filling gas is typically in the range 0.5 - 2 mTorr,
- the steady equilibrium field is switched on and, if required, the preionization system,

- after sufficient time has elapsed for the equilibrium field to rise to a steady value, the RF generators which provide the RMF are triggered. In many experiments, the equilibrium field and the RMF are triggered simultaneously. The rotating field both increases the percentage ionization of the filling gas and generates the plasma current,
- the RF supplies are switched off after a pulse of ~ 40 msec duration,
- the equilibrium field is switched off.

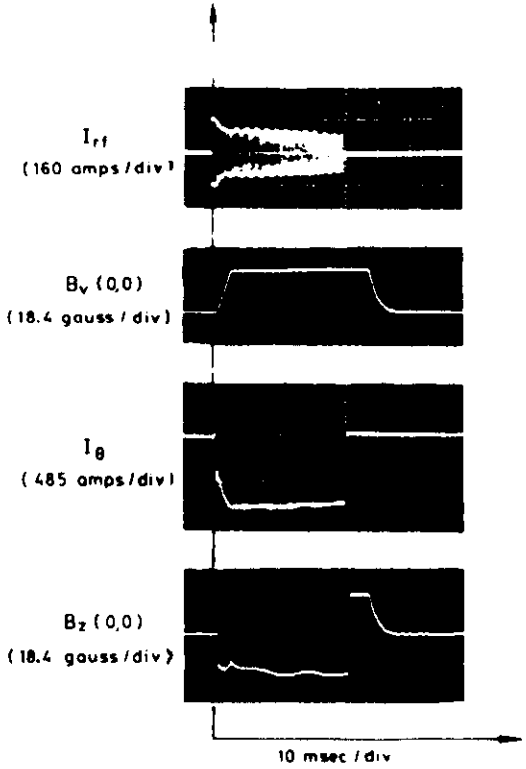

Fig. 10 I_{rf}, $B_v(0,0)$, I_θ and $B_z(0,0)$ signals for a rotamak discharge [12] (Quantities defined in text).

Fig. 10 shows some measurements made on a rotamak discharge with a filling pressure of 0.3 mTorr H_2.[12] The envelope of one of the two RF current pulses utilized, I_{rf} (RF frequency: 1.0 MHz); the initially imposed equilibrium field, $B_v(0,0)$, measured at r = 0, z = 0 *in the absence of plasma*; the steady plasma current driven by the RMF, I_θ; and the z-component of the steady magnetic field at r = 0, z = 0, $B_z(0,0)$, *measured during the discharge* are shown. The slight ripple on the I_{rf} waveform is an artifact of the measuring system and is to be ignored. The I_θ trace indicates that 1050 amps of toroidal plasma current is driven reproducibly for the chosen initial conditions. (Two I_θ traces have been overlayed in Fig. 10). A comparison of the $B_v(0,0)$ and $B_z(0,0)$ traces shows that the driven current brings about a period of field reversal at the centre of the discharge vessel thus indicating that a compact torus configuration has been generated. The termination of the current pulse and the period of field reversal (after which $B_z(0,0)$ reverts to the $B_v(0,0)$ value) coincides with the end of the rotating field pulse. We re-emphasize that the observation of field reversal is a firm and useful indication that the desired configuration has indeed been produced. The set of measurements presented in Fig. 10 are the ones which should be initially undertaken in any new rotamak experiment.

In a recent publication[13], the ANSTO group have shown the manner in which a number of parameters evolve with time in a typical rotamak discharge. For the example shown in Fig. 11, the filling pressure was 1.1 mTorr H_2 and the various parameters are:

- I_{VF} - the current through the equilibrium field coils. The value of $B_v(0,0)$ corresponding to the 'flat-top' of this current pulse is 35 gauss,
- I_{tor} - driven toroidal plasma current (designated I_θ elsewhere in this paper),
- I_1, I_2 - peak RF currents in the RMF coils,
- Phase - the phase angle between the RF currents, I_1 and I_2,
- P_{rf} - RF input power to the plasma,
- $\bar{n}_e$ - line-averaged electron density,

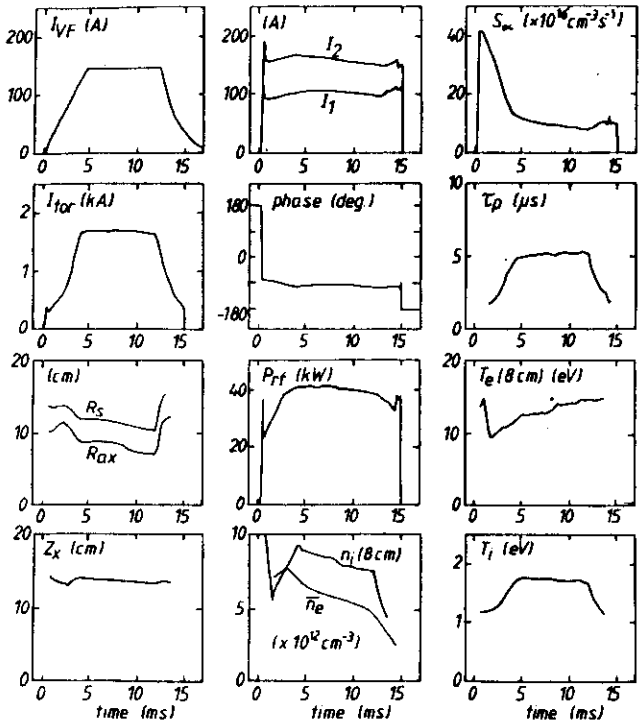

Fig. 11 Time development of a typical rotamak discharge[13] (Quantities defined in text)

- n_i (8 cm) - local ion density at the magnetic axis,
- T_e (8 cm) - local electron temperature at the magnetic axis,
- T_i - ion temperature,
- R_s, R_{ax}, Z_x - positions of the separatrix (in the z = 0 plane), the magnetic axis and the neutral point, respectively,
- S_α - average H_α emission-rate,
- τ_p - particle confinement time.

The experiment was conducted in a spherical pyrex vessel of radius 14 cm.

During the 'flat-top' stage of the discharge, the driven plasma current, I_{tor}, remains constant even though the RF input power decreases slowly during this time. As the RF input power decreases, the position of the separatrix, R_s, moves radially inwards to, presumably, reduce the power loss from the plasma to the vessel wall. Other experiments consistently indicate this sensitive relationship between the separatrix position and the RF input power.

The electron density decreases continuously through the 'flat-top' period while the electron temperature increases, keeping the electron pressure roughly constant.

The reader is referred to the paper by Collins et al.[13] for a complete discussion of their rotamak scaling experiments. Fig. 11 is presented here only to give an indication of the values which are attained by the various parameters in a typical contemporary rotamak device.

A noteworthy feature of the rotamak discharge is its remarkable reproducibility. In some experiments, a discharge made with a given set of initial conditions has been observed to be reproducible over a series of ~ 10,000 successive shots! An indication of this reproducibility is given in Fig. 12(a) and (b). Fig. 12(a) shows the quantity we have denoted by $B_v(0,0)$ and Fig. 12(b) shows the corresponding $B_z(0,0)$, taken during a rotamak discharge[3]. The reversal of the $B_v(0,0)$ field is very reproducible; measurement from 10 shots are overlayed in Fig. 12(b).

Conventional MHD stability theory predicts that the rotamak configuration is unstable on the microsecond timescale. The reason for the observed stability of the rotamak is not known at present and remains an open question. Some unpublished calculations by Brotherton-Ratcliffe and Bertram do indicate that, in addition to driving the desired toroidal plasma current, the applied rotating magnetic field has a stabilizing influence.

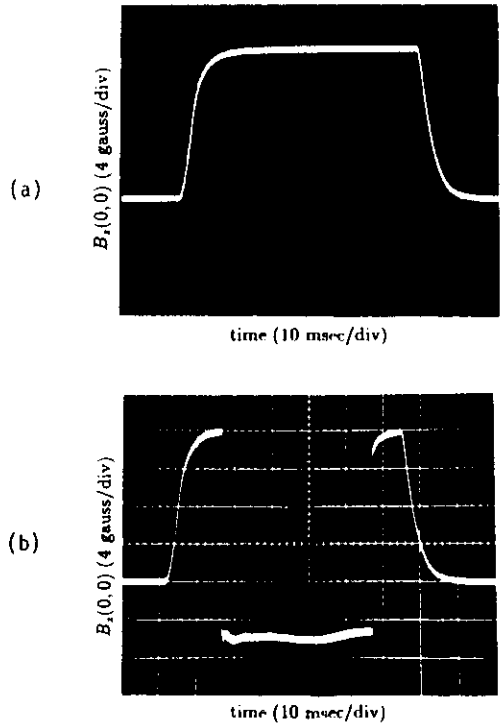

Fig. 12 Reversal of $B_v(0,0)$ in a rotamak discharge[3]
(a) $B_v(0,0)$
(b) $B_z(0,0)$; measurements from 10 successive discharges are overlayed.

4.2 The Determination of the Magnetic Structure of a Rotamak Discharge.

At any instant of time, the lines of the total magnetic field (steady plus rotating) in a rotamak discharge are open. However, the steady (or time-averaged) part of the total field forms the closed field line system shown in Fig. 1. By now, there is ample experimental evidence[10,13] to indicate that the plasma particles are confined by the steady magnetic field. (The position is not yet clear with respect to the confinement of plasma energy). The determination of the steady magnetic field configuration for a given rotamak discharge thus constitutes an important task in rotamak research.

As mentioned earlier in this paper, the steady components of the magnetic field are measured by means of Hall probes which, for the densities and temperatures encountered in contemporary rotamak experiments, can be completely inserted into the plasma.

For the purpose of illustration, we now present the results of an investigation carried out by Knight[4] on a highly elongated rotamak discharge. A schematic diagram of the experimental apparatus is shown in Fig. 13(a), while the magnetic fields produced by these coil structures are depicted in Fig. 13(b).

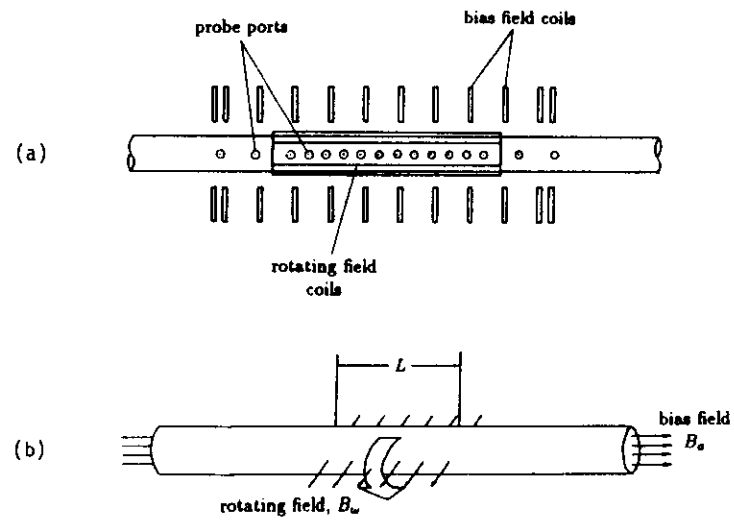

Fig. 13 Highly prolate rotamak experiment[4]
(a) Schematic diagram of apparatus
(b) Magnetic fields produced by coil structures.

A set of coils located along the length of the discharge tube (pyrex cylinder of minor diameter 10.0 cm) was used to generate a steady axial (z-direction) magnetic field, B_a. Axially directed rotating field coils generated a transverse rotating field over a limited length, L (= 50 cm), of the tube. The application of the RMF both ionized the gas fill and generated a quasi-steady azimuthal plasma current. The sense of rotation of the RMF was chosen so that the steady axial magnetic field produced by the plasma current was oppositely directed to B_a. If large enough, it was capable of reversing B_a and of thus forming a highly prolate compact torus whose length (between the neutral points) was a substantial fraction of L.

A glass tube could be inserted across the diameter of the discharge tube at any one of sixteen axial positions (see Fig. 13(a)). To minimize the disturbance to the plasma when taking magnetic field data, only one diametrical guide tube was inserted at a time.

A Hall probe was used to measure the z-component of the steady magnetic field across diameters of the discharge vessel at a number of z-positions. The probe was moved radially in increments of 5 mm. A discharge was produced with the probe at each radial position and the digitized data was stored on disk. Data was subsequently selected at fixed time steps to produce output in the form of $B_z(r)$ at fixed z-positions.

Fig. 14 shows the radial profiles of $B_z(r)$ at each of fourteen chosen z-positions and at a given time in a discharge made with 8 mTorr of argon as the filling gas; the crosses are the measured values. The experimental data was smoothed by fitting a symmetric, two-dimensional polynomial surface (in r and z) of the following form to the data:

$$B_z(r,z) = \sum_{\alpha=0}^{N_1} \sum_{\beta=0}^{N_2} a_{\alpha\beta}\, r^{2\alpha}\, z^{2\beta}$$

Details of the fitting routine can be found in Knight[4]. The solid curves in Fig. 14 are radial cuts of the fitted surface at the given z-position. The polynomial order for this case was $N_1 = 6$ and $N_2 = 4$.

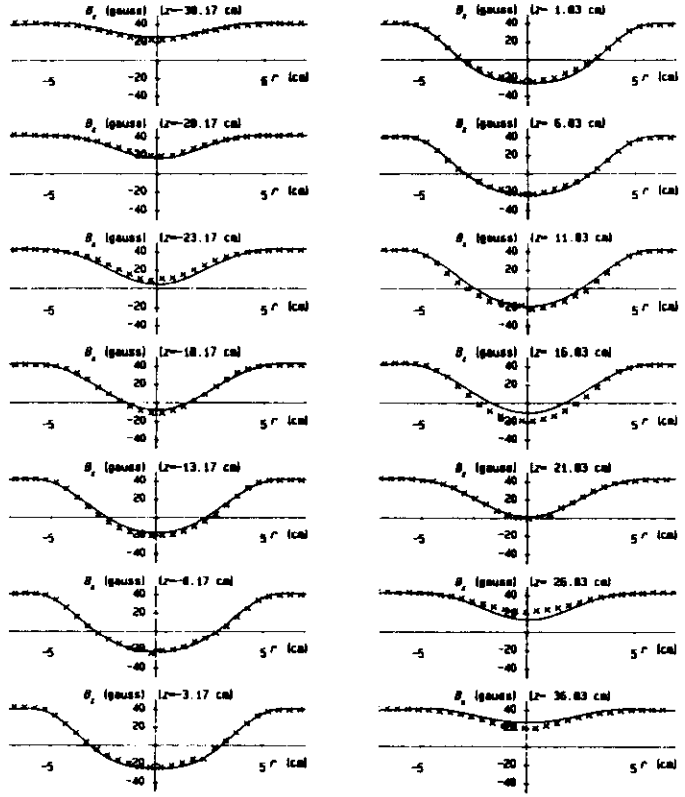

Fig. 14 Comparison of the measured $B_z(r)$ profiles with cuts in the fitted polynomial surface.

Given that the surface is being fitted to *all* the data points (392 total) at once, the fit is excellent.

The polynomial coefficients which were obtained by this fitting procedure were then used to derive the poloidal flux,

$$\Psi(r,z) = \int_0^r 2\pi\, r'\, B_z(r',z)\, dr'$$

$$= 2\alpha \sum_{\alpha} \sum_{\beta} \frac{a_{\alpha\beta}}{2\alpha + 2}\, r^{2\alpha+2}\, z^{2\beta}$$

and the azimuthal current density,

$$j_\theta(r,z) = -\frac{1}{\mu_0} \sum_{\alpha} \sum_{\beta} a_{\alpha\beta} \left[\frac{2\beta(2\beta-1)}{2\alpha+2}\, r^{2\alpha+1}\, z^{2\beta-2} + 2\alpha\, r^{2\alpha-1}\, z^{2\beta}\right] .$$

Derivation of the current density normally involves calculating derivatives of B_z and it is well-known that numerical differentiation of experimental data is extremely sensitive to small errors in the measurements. Fitting a smooth polynomial surface to the data in the manner just described circumvents this problem.

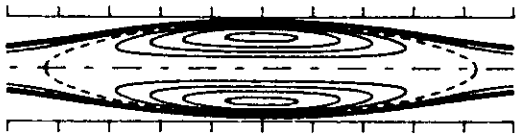

Fig. 15 Contours of poloidal flux derived from data shown in Fig. 14. (Contour spacing : 1×10^{-6} Wb)

Fig. 15 shows the poloidal flux contours (contours of equal values of Ψ) derived from the data presented in Fig. 14. The broken contour is the separatrix and corresponds to the surface of zero flux; it also separates regions of closed and open field lines. The magnetic configuration produced in this particular rotamak experiment was that of a highly elongated (prolate) compact torus.

The fitting of two-dimensional polynomial surfaces to magnetic probe data has become standard practice in rotamak research and its use has been extended to the analysis of number density and temperature data obtained with electric probes (see, e.g. Fig. 16(a) and (b)).

4.3 Plasma Parameters

Typical plasma parameters obtained in contemporary rotamak experiments are:

$$n_e = 10^{18} - 10^{19}\ m^{-3} ,$$

$$T_e = 10 - 20\ eV ,$$

$$T_i = 1 - 2\ eV$$

and $$\tau_p \sim 5\ \mu sec.$$

These modest values need to be improved before an assessment can be made of the potential of the rotamak as a fusion device. This problem will be addressed in Section 5.

4.4 Rotamak Equilibria

In the companion paper a simple and useful axisymmetric MHD equilibrium, the Solov'ev solution of the Grad-Shafranov equation, was described. An example of its application will now be presented.

In section 4.2, details of the magnetic configuration generated in an experiment by Knight[4] were presented and, in particular, contours of $\Psi(r,z)$ were shown (Fig. 15). Knight also measured the electron number density, n_e, and temperature, T_e, in his experiment and the measured contours of these quantities are shown in Fig. 16(a) and (b). Fig. 16(c) shows the derived contours of electron pressure, $p_e = n_e k T_e$.

It will be recalled that in order to solve the Grad-Shafranov equation, one requires to know the functional dependence of the total plasma pressure, p, on the stream function, ψ. Now, p is the sum of the electron and ion pressures,

$$p = p_e + p_i .$$

We will neglect the ion contribution to the total pressure and write:

$$p = p_e .$$

Justification for this assumption can be found in rotamak power balance

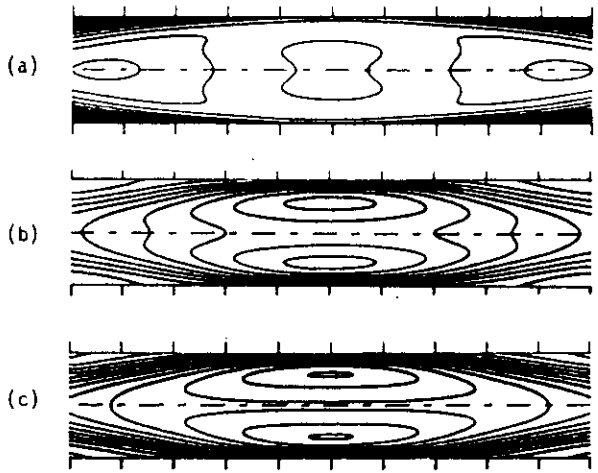

Fig. 16 Contours of (a) electron temperature (contour spacing : 0.5 eV)
(b) electron density (contour spacing : 1×10^{18} m^{-3})
(c) electron pressure (contour spacing : 1 Pa)

calculations undertaken by Donnelly et al.[14)]

The functional relationship between p (= p_e) and ψ $\left(= \frac{\Psi}{2\pi}\right)$ was determined in the following manner. The two-dimensional polynomial fits to p_e and Ψ were used to calculate p_e and ψ over a grid of points in the coordinate space of r and z. Each (r,z) point then defined a pair of numbers (ψ, p_e) which could be plotted. The result is shown in Fig. 17. Here, the points for fixed z-positions have been joined. In this way a family of curves corresponding to different z-values is obtained. Negative values of ψ correspond to the region of closed flux contours and positive values correspond to open flux contours. To a reasonably good approximation, p_e is *experimentally observed* to be a linear function of ψ. A line of best fit is shown in Fig. 17.

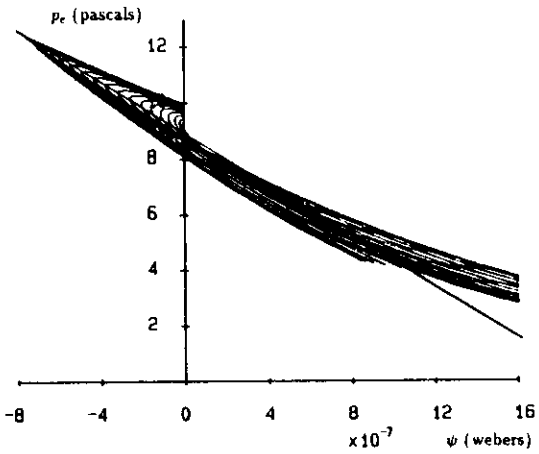

Fig. 17 Electron pressure, p_e, plotted against the stream function, ψ.

The fact that $p_e \sim \psi$ is a happy circumstance, for it means that the Solov'ev solution to the Grad-Shafranov equation,

$$\psi(r,z) = \frac{B_o r^2}{2R^2}\left(r^2 + \alpha^2 z^2 - R^2\right) ,$$

is applicable. Here, R is the radius of the separatrix in the z = 0 plane, $B_o = |B_z(0,0)|$ and $\alpha = R/z_x$, where z_x is the position of the neutral point on the z-axis.

Substitution of this solution into the Grad-Shafranov equation yields:

$$p = C\psi + p_o ,$$

where

$$C = -\frac{4B_o}{\mu_o R^2}\left(1 + \frac{\alpha^2}{4}\right)$$

and where $p = p_o$ when $\psi = 0$.

Since B_o, R and α were experimentally determined quantities, it

was possible to compute a value for C from the above expression and, then, compare it directly with the slope of the straight line fit shown in Fig. 17.

From the measurements:

$$B_o = 2.5 \times 10^{-3} \text{ Wb m}^{-2}$$

$$R = 4.3 \text{ cm}$$

$$Z_x = 21.6 \text{ cm (and, hence, } \alpha = 0.2) .$$

Substitution of these values yields a theoretical value of

$$C^{th} = -4.3 \times 10^{6} \text{ Pa Wb}^{-1} .$$

This is to be compared with the slope of the best line fit in Fig. 17 which is:

$$C^{exp} = -4.6 \times 10^{6} \text{ Pa Wb}^{-1} .$$

The agreement is excellent and confirms that the Solov'ev solution provides a good quantitative description of the observed equilibrium.

Fig. 17 shows clearly that the plasma generated in the Knight experiment was not completely magnetically confined. In fact, only 3.4 Pa was confined magnetically, the pressure on the separatrix (p_o) being 8.9 Pa. This situation arises, to varying degrees, in all rotamak experiments - and, let it be said, in other compact torus experiments as well.

In many rotamak experiments it is found that there is a linear dependence of the driven toroidal current, I_{tor}, on the initially applied equilibrium field, B_z^{vac} (designated $B_v(0,0)$ elsewhere in this paper). As an example of this, Fig. 18 shows the measured dependence reported by the ANSTO group in their latest publication.[13)]

For a spherical equilibrium ($\alpha = 1$), the Solov'ev solution predicts that:

$$\frac{I_{tor}}{B_z^{vac}} = \frac{5R}{\mu_o} .$$

That is, it predicts a linear relationship between I_{tor} and B_z^{vac} provided R is constant. If we assume that R = 14 cm (the radius of their vacuum vessel) and is fixed, then:

$$\frac{I_{tor}}{B_z^{vac}} = 5.6 \times 10^{5} \text{ amps - Wb}^{-1} \text{ m}^2$$

A straight line having this slope is shown in Fig. 18. Again we see

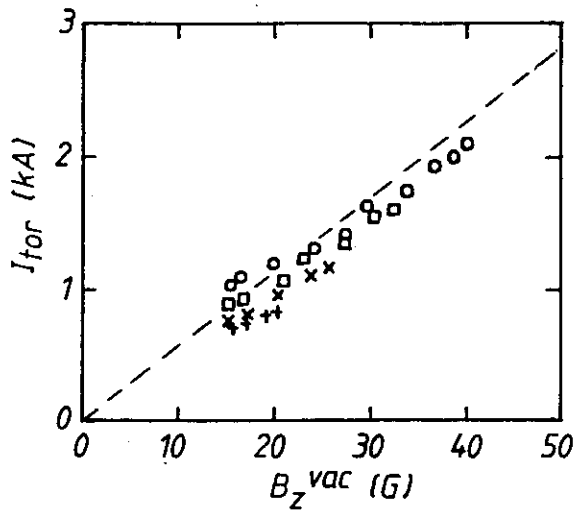

Fig. 18 Measured dependence of I_{tor} on B_z^{vac} . Dotted line is the prediction of the Solov'ev solution.

that the Solov'ev solution provides a good description of observed rotamak equilibria.

5. FUTURE PLANS IN ROTAMAK RESEARCH

The plasma parameters achieved to date in rotamak discharges can at best be described as modest. In hydrogen rotamak discharges one obtains, typically, $n_e \sim 5 \times 10^{18} \text{ m}^{-3}$ and $T_e \sim 10 - 15$ eV. Even so, measurements show that the $\underline{j} \times \underline{B}$ forces which are present can only confine about 50% of the peak plasma pressure in the present generation of rotamak devices; the rest of the plasma pressure is taken up by the vessel wall. This circumstance can be understood as follows.

When a rotamak discharge is initiated by the application of an RF rotating magnetic field, two things occur

- a plasma is formed which exerts a certain pressure on its surroundings
- a plasma current is driven and the $\underline{j} \times \underline{B}$ forces associated with it assist in maintaining the pressure gradient of the plasma.

There is no a priori reason to expect that the radial $\underline{j} \times \underline{B}$ force will completely confine the plasma pressure which is generated by the application of the RF fields. What is observed in present-day rotamak experiments is that the plasma pressure is at least double that which can be held by the magnetic forces acting alone. Improved magnetic confinement and, hence, improved plasma parameters, will only come about if we can increase the value of the driven current. In present experiments, the filling gas is not fully ionized and any attempt to increase the driven current by increasing the input power only results, in the first instance, in an increased percentage ionization, the electron temperature being clamped at a nearly constant, low value (as in a change of phase). In these circumstances, the value of the electron-ion collision frequency, ν_{ei} (which is proportional to $n_e/T_e^{3/2}$) is high and the driven current will only increase slowly with increased RF input power.

We can confidently anticipate that if the RF input power is greatly increased, the filling gas will approach full ionization and the electron temperature will significantly increase. The value of ν_{ei} will start to decrease at this stage (since $n_e \sim$ constant and T_e is increasing) and the current drive mechanism will become much more efficient (recall that the amount of driven current is a strongly non-linear function of $1/\nu_{ei}$).

What value of RF input power will give full ionization in present-day rotamak experiments with hydrogen? A zero-dimensional, time-dependent model has been used to evaluate the level of RF power which is required to significantly improve the low ionization levels and electron temperatures which characterize our present experiments. On the basis of these calculations, two new RF output stages, each capable of delivering 400 kW in a 40 msec pulse (RF frequency: 0.5 → 1.0 MHz) are being constructed at Flinders University. These stages are now ready for use and a new series of rotamak experiments will be started in a 60 cm (diameter) × 80 cm (length) glass cylinder in mid-1989.

ACKNOWLEDGEMENTS

The Rotamak project is ten years old this year (1989). During this past decade, I have been fortunate to be associated with two fine groups of people, the rotamak researchers at ANSTO (Lucas Heights, N.S.W.) and their colleagues here at my home institution, Flinders University, S.A. It has been a pleasure to work with these people and I wish to express my special thanks to them at this time.

REFERENCES

1) Jones, I.R., Flinders University Report No. FUPH-R-151 (February 1979). NTIS-PB85-133858.

2) Hugrass, W.N., Jones, I.R., McKenna, K.F., Phillips, M.G.R., Storer, R.G. and Tuczek, H., Phys. Rev. Lett. 44, 1676 (1980).

3) Kirolous, H.A., Brotherton-Ratcliffe, D. and Jones, I.R., Plasma Phys. Contr. Fusion 31, 79 (1989).

4) Knight, A.J., Ph.D. Thesis (Flinders University) February 1988.

5) Stephan, L.G., Ph.D. Thesis (Flinders University) September 1983.

6) Hugrass, W.N., Aust. J. Phys. 39, 513 (1986).

7) Hugrass, W.N., Jones, I.R. and Phillips, M.G.R., J. Phys. E: Sci. Instrum., 13, 276 (1980).

8) Durance, G. and Jones, I.R., Phys. Fluids 29, 1196 (1986).

9) Jones, I.R., Turley, M.D.E., Wedding, J.E., Durance, G., Hogg, G.R. and Tendys, J., Aust. J. Phys., 40, 157 (1987).

10) Durance, G., Hogg, G.R., Tendys, J. and Watterson, P.A., Plasma Phys. Contr. Fusion 29, 227 (1987).

11) Tendys, J., Rev. Sci. Instrum. 58, 315 (1987).

12) Jones, I.R., Proc. Invited Papers 1984 International Conference on Plasma Physics, Lausanne, Switzerland, June 27 - July 3, 1984. Vol. I, p.473.

13) Collins, G.A., Durance, G. and Tendys, J., Plasma Phys. Contr. Fusion 31, 651 (1989).

14) Donnelly, I.J., Rose, E.K. and Cook, J.L., Aust. J. Phys., 40, 393 (1987).